Investigation of Some Parameters Which Affects Into The Efficiency of Quantum Dot Intermediate Band Solar Cell

Abou El[*], Maaty M. Aly[**‡]

*Researcher, Dept. of Power Electronics and Energy Conversion, ERI, NRCB, Egypt

**Assistant professor, Dept. of Computer Engineering, College of Computer, Qassim University, KSA

abouelmaaty67@gmail.com

‡Corresponding Author: Abou El, e-mail: abouelmaaty67@gmail.com

Abstract- In this paper, Quantum dots intermediate band solar cell (QDIBSC) is used to the enhancement of the power conversion efficiency of solar cell. The main advantage of this type is that it preserves large open-circuit voltage with increasing the produced photocurrent in the solar cell. For a best efficiency of one-intermediate band solar cell (one-IBSC), the induced detailed balance efficiency is determined as a function of changing locations of intermediate-band (IB) by using the blackbody. The QDs have the ability to confirm the chosen higher efficiency by assigning the appropriate values of quantum dot width size (QDW) and barrier thickness (BT). It means that the best location of IB in solar cell is realized. The results show that to obtain the maximum power conversion efficiency of QDIBSC, the QDWs and BTs for nanostructured model (Al0.4Ga0.6As/In0.42Ga0.58As) are limited by a surface contour. The highest power efficiencies in this located contour are 45.32% and 62.81% for QDWs = (1.60 nm, 1.64 nm) and BTs = (1.98 nm, 1.94 nm) for 1 sun and maximum light concentrations; respectively.

Keywords-Quantum Dots Width, Barrier Thickness, Intermediate Band, Efficiency, Nanostructured Solar Cell.

1. Introduction

Throughout the past decades, the whole world started to feel the seriousness of the deficiency in the fossil fuel. Therefore, a large number of researchers around the world began to research and study the alternative energy to compensate the loss in traditional energy. Solar energy is one of the important options for alternative energy and improving this technology can clearly reduce the problem of energy in the world [1-5]. Consequently, a number of researchers at Nano-power Research Laboratories and others focus on the improvement of the power conversion efficiency of solar cells by using nanostructures with suitably adjusted properties [6-8]. The new proposed concepts are called third-generation solar cell, such as hot carrier cells, tandem cells, and intermediate-band cells [4, 7, 9-12]. The intermediate energy bands are established within a forbidden gap of a bulk semiconductor material when a superlattice low-dimensional nanostructure (quantum well, wire, and dot (QW, QR, and QD respectively)) of other semiconductors material injected within a bulk semiconductor material [13-15]. This structure is called heterostructure and it allows for the proper operation of IBSC. For QW and QR heterostructures, the photogenerated charge carriers will lose energy through thermalization due to the high density of states available in the in-plane and longitudinal direction; respectively [16]. Also, the Fermi level will not split into the number of bands, but it will split into two levels similar to the traditional solar cell. Moreover, the lowest intermediate band will act as the conduction band and the heterostructure will behave like the traditional solar cell [17-18]. For QDs heterostructure, it will provide zero density of states between the excited bands due to the discrete energy spectrum; thus the thermalization is reduced. Each band is thermally isolated; therefore the Fermi energy level will split into the number of bands and charge concentration in each band is described by its own chemical potential as required for improving IBSC operation [16, 19]. Fig. 1(a) shows QDIBSC with the barrier material surrounding the QDs. QDs are made of the materials such as Ge, InAs, InAsN,..etc., they have smaller bandgap energy than the bulk materials such as Si, GaAs, GaAsN,..etc [4, 6, 7, 10, 11]. The superlattice structure is an array of closely

spaced QDs, therefore a sufficient amount of wavevectors overlapped to form the intermediate energy bands as shown in Fig. 1(b) [8, 12]. These bands are critical in the nanostructured solar cell because they allow the absorption of low energy photons in addition to the normal absorbed photons processes. Therefore, the efficiency is improved, as a result of increasing the generated photocurrent [20]. The

organization of this paper includes the following parts. Part II includes the related work for QDIBSC. The analyses of the mathematical model are described in Part III. The one-intermediate band solar cell is discussed in Part IV. The quantum dot intermediate band solar cell at different QDs width sizes and barrier thickness is described in Part V. Finally, Part VI is the conclusions of this article.
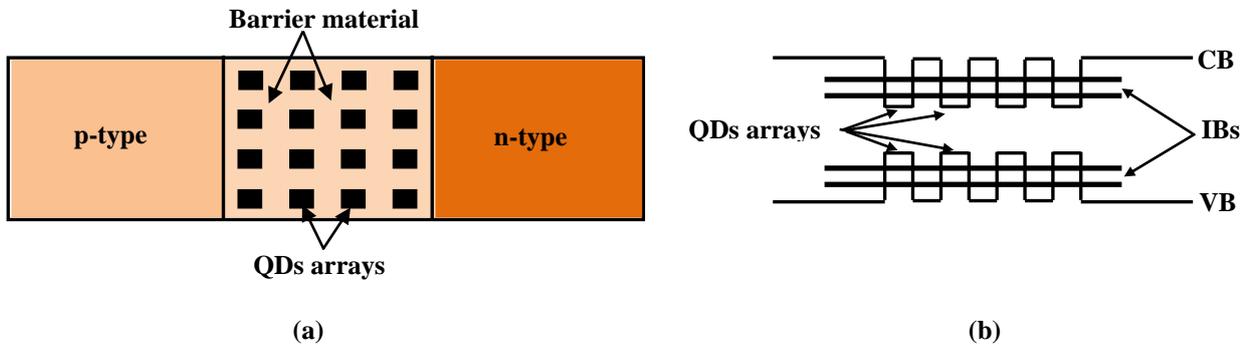

Fig. 1. (a) Schematic diagram of the QDs inside a bulk semiconductor of larger bandgap **(b)** Intermediate energy bands of an array of QDs

2. Related Work

Since 1997, IBSC have received the attention of a large number of research groups due to the potential of the IB to increase the power conversion efficiency of solar cell devices from 41% to 63% under maximum light concentration [21]. The key working principle of the IBSC have been demonstrated in a InAs/GaAs quantum dot solar cell [22], though so far to the knowledge of the author no net increase of the efficiency has been shown by an IB device respect to a device with the same characteristics but lacking the IB. Reviews of the topic can be found in references [23, 24]. Many authors report strong enhancement of the photocurrent [25] due to subbandgap absorption, and even large increase in efficiency compared to reference devices [2]. Sablon et al. [2] fabricated InAs/GaAs quantum dot solar cells and reported a large increase in current without significant voltage degradation. This field has expanded a lot, as much to propose materials that show an IB without the insertion of nanostructures [26, 27]. Other models proposed also include space-charge and other recombination effects to best fit the experimental data [28, 29]. Recent progress has also been made with the growth of InAs/GaAs quantum dot solar cells with MOCVD [4] and even transfer to flexible substrates by epitaxial lift-off [30]. A possible limitation to this technology comes from strain-induced defects that can generate in the QD layers [31], and eventually limit the number of layers that can be grown. Higher densities of QDs in strain compensated materials have been proposed and realized [32, 33]. An interesting feature of strain-compensated QD multilayer's is the self-ordering effect observed in multilayered samples

[34]. This ordering may lead to the formation of a mini-band that would serve as the perfect IB as theorized in [21].

3. Mathematical Model Analyses

The principle of a mathematical model to describe the operation of a solar cell is built on using the sun as a blackbody. The generalization of Planck's radiation law for blackbody and solar radiation is [5, 14, 16]

$$S_R = \frac{2\pi hc^2}{\lambda^5} \frac{1}{e^{((hc/\lambda-\mu)/kT)}-1} \tag{1}$$

Where S_R is a solar spectrum, λ is wavelength of light, h is Planck's constant, c is the speed of light, μ is the chemical potential, k is Boltzmann's constant, and T is the temperature of a blackbody. From the Roosbroeck-Shockley equation, the flux of photons (φ) absorbed in or emitted from the semiconductor is given by [19]

$$\varphi(\lambda_a, \lambda_b, T, \mu) = \int_{\lambda_a}^{\lambda_b} S_R \, d\lambda \tag{2}$$

Where λ_a and λ_b are the lower and upper wavelengths of the light at the energy limits of the photo flux. When handling the sun as an ideal blackbody and the solar absorption of a semiconductor is limited by the bandgap energy E_g, the flux of photons absorbed at the sun's surface (φ_s) is

$$\varphi_s(0, \lambda_g, T_s, 0) = \int_0^{\lambda_g} \frac{2\pi hc^2}{\lambda^5} \frac{1}{e^{((hc/\lambda-\mu)/kT_s)}-1} d\lambda \tag{3}$$

Where λ_g is the wavelength of light at the bandgap energy of the solar semiconductor, T_s is the temperature of the sun, 6000K. The photon flux absorbed by the solar cell, φ_{ssc}, is shown in Fig. 2 and denoted by:

$$\varphi_{ssc} = \varphi_s \times f_s \tag{4}$$

Where $f_s = 2.1646 \times 10^{-5}$ is called geometric parameter [16].

Similarly, the solar cell may be considered as an ideal blackbody at temperature $T_c = 300K$. Then, a photon emission from the solar cell with a flux φ_{sc} is emitted when an electron-hole pair is directly recombined. The flux φ_{sc} is the same as in Equation 3, but the surface sun temperature, T_s is replaced by the surface solar cell temperature, T_c. According to the Shockley-Queisser model, the current density (j) of the solar cell device can be written as [35]

$$j = q[c_s f_s \varphi_s(0, \lambda_g, T_s, 0) + (1 - c_s f_s)\varphi_{sc}(0, \lambda_g, T_c, 0) - \varphi_{sc}(0, \lambda_g, T_c, \mu)] \qquad (5)$$

Where c_s is the light concentration on a solar cell and it is called the number of suns, i.e., 1 sun means that $c_s = 1$ at the surface of the Earth's atmosphere and 46198 suns mean that $c_s = 1/f_s$ or maximum light concentration at the surface of the sun's. The chemical potential of solar photons (μ) is equal to the applied bias (qV) which it is equal to the number of splitting in the quasi-Fermi energy levels, where q is electron charge and V is the applied voltage of the solar cell. This equation represents the detailed balance formula; it directly provides the current-voltage characteristics of a solar cell. Also, the solar power conversion efficiency can be directly calculated.
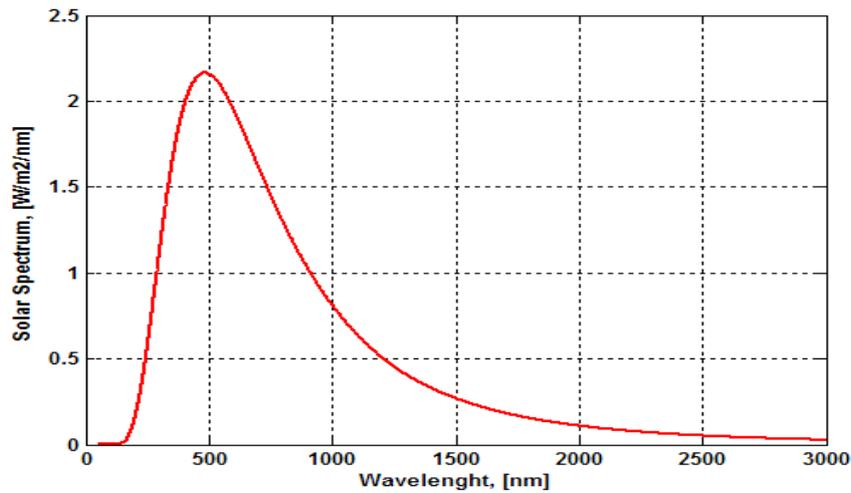

Fig. 2. Solar spectrum versus wavelength at blackbody

4. One-Intermediate Band Solar Cell

The main challenge in improving the performance of the traditional solar cells is the case where the increasing output current decreases the output voltage and vice versa. A number of articles discussed how to handle this problem by making a tradeoff between the materials used in the manufacturing of solar cells. The traditional solar cell would only be able to absorb photons with energy equal to or greater than the energy between conduction and valence bands (E_{CV}). For the nanostructured solar cell, new bands are located at an intermediate level (E_I) between conduction and valence bands. These bands increase the absorption of photons that lead to the increased performance of this design when compared to the traditional solar cell. To study the mathematical model of this type, the following assumptions are necessary [5, 12, 36, 37]:

i. There is no overlap of energy transitions for a given photon energy; i.e., if a photon may energetically induce a transition from one band to another, then all photons of the same energy will only cause that particular transition.

ii. Electrons enter the IB only when transferred from the valence band (VB) and they leave only to the conduction band (CB).

iii. The difference in chemical potentials between any two bands causes only the difference between the quasi-Fermi levels of these bands.

In the following, the study will concern a one-IBSC taking into account the considered assumptions. It has three transitions of electrons between bands. (1) The standard effect of an electronic transition across the traditional bandgap E_{CV} generates the current density (j_{CV}). (2) The effect of the intermediate to conduction band transition (E_{CI}) produces the current density (j_{CI}). (3) The transition between valence and intermediate bands (E_{IV}) will produce a current density (j_{IV}). One can notice that j_{CI} must be equal to the current density j_{IV}. The two energy intermediate band transitions, E_{CI} and E_{IV} are independent of each other; however, the traditional bandgap E_{CV} is a function of these bands. Thus, the three generated current densities are

$$j_{CV} = q[c_s f_s \varphi_s(0, \lambda_{CV}, T_s, 0) + (1 - c_s f_s)\varphi_{sc}(0, \lambda_{CV}, T_c, 0) - \varphi_{sc}(0, \lambda_{CV}, T_c, \mu)]$$

$$j_{CI} = q[c_s f_s \varphi_s(\lambda_{CI}, \lambda_{IV}, T_s, 0) + (1 - c_s f_s)\varphi_{sc}(\lambda_{CI}, \lambda_{IV}, T_c, 0) - \varphi_{sc}(\lambda_{CI}, \lambda_{IV}, T_c, \mu_{CI})]$$

$$(6) \qquad j_{IV} = q[c_s f_s \varphi_s(\lambda_{IV}, \lambda_{CV}, T_s, 0) + (1 - c_s f_s)\varphi_{sc}(\lambda_{IV}, \lambda_{CV}, T_c, 0) - \varphi_{sc}(\lambda_{IV}, \lambda_{CV}, T_c, \mu_{IV})]$$

Since the current densities j_{CI} and j_{IV} must be equal, therefore the total current density $j_T = j_{CV} + j_{CI}$. As in previous analyses [13, 16, 38], the chemical potential of photons is

equal to the applied bias ($\mu = qV = \mu_{CI} + \mu_{IV}$), which is equal to the number of splitting in the quasi-Fermi energy levels. Fig.3 analyzes the detailed balance efficiency under

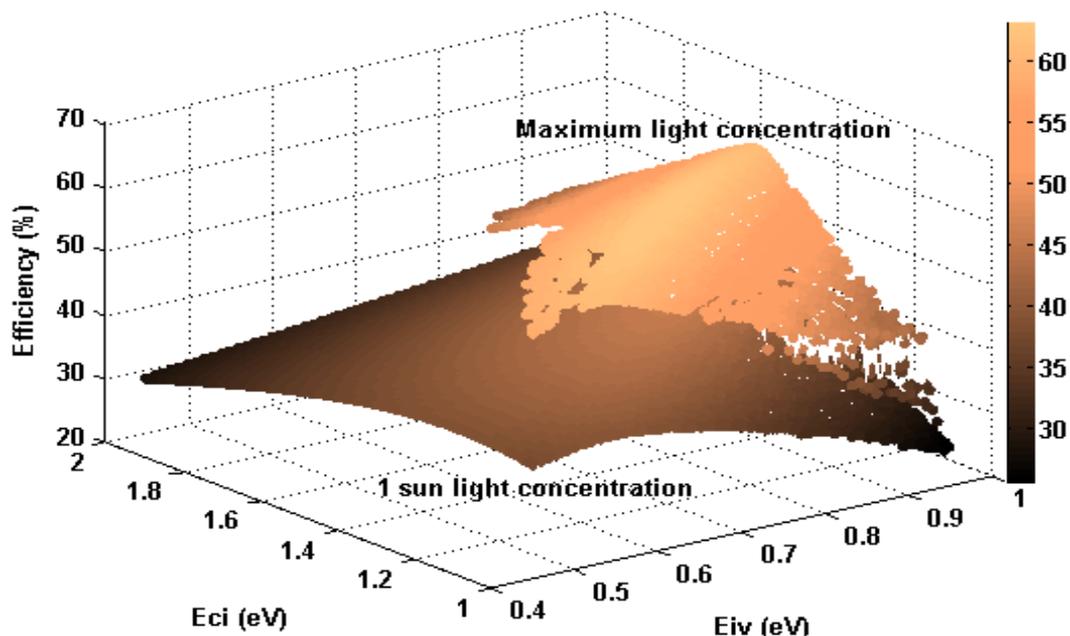blackbody solar spectrum at 1 sun and maximum light concentrations.

Fig. 3. Detailed balance efficiency of one-IBSC varies with the place of IB between the CB and VB at blackbody spectrum under 1 sun, and maximum light concentrations

The place of one-IB that achieves the maximum power efficiency can be recognized by changing the limited values of bandgap energies E_{IV} and E_{CI}. The maximum efficiency is reached to 46.74% which corresponds to the optimum intermediate energy band position at $E_{IV} = 0.93$eV and $E_{CI} = 1.5$eV; the total bandgap energy $E_{CV} = 2.43$eV. When the

light concentration is increased to a maximum, the maximum efficiency is increased to 63.13% and the optimum intermediate energy band position in this case will be $E_{IV} = 0.72$eV and $E_{CI} = 1.25$eV; $E_{CV} = 1.97$eV, these determined values also shown in Table 1.

Table 1. Summarizes the maximum efficiency, optimum bandgap, and IB for any one-IBSC at 1 sun and maximum light concentrations for the blackbody spectrum

Solar Spectrum	1 sun light concentration				Max. light concentration			
	Max. Efficiency (%)	Opt. Bandgaps (eV)			Max. Efficiency (%)	Opt. Bandgaps (eV)		
		E_{CI}	E_{IV}	E_{CV}		E_{CI}	E_{IV}	E_{CV}
Blackbody	46.74	1.50	0.93	2.43	63.13	1.25	0.72	1.97

One can notice that, in the case of maximum light concentration, the IB energies, E_{CI} and E_{IV}, and then corresponding bandgap energy, E_{CV}, are decreased. Practically, there is a critical note should be taken into consideration that is the order of the energy intermediate bands E_{CI} and E_{IV} does not affect the efficiency of the one-IBSC. Because of the efficiency depends only on the transition energies themselves [16]. For example, the theoretical efficiency is equal to 63.13% under maximum

light concentration when $E_{CI} = 1.25$eV and $E_{IV} = 0.72$eV. However, the same result is also achieved when $E_{CI} = 0.72$eV and $E_{IV} = 1.25$eV, therefore the order of the transition energies is unimportant. From Fig. 3, it is clear that in the case of the maximum light concentration, not all the values of E_{IV} and E_{CI} are included in the 3D curve, which indicates the difficulty to realize the transition energies condition for the same values of induced currents; $j_{CI} = j_{IV}$. This is the reason not all efficiency values are dominated. For further declaration, the light concentration range is scanned as shown in Fig. 4.
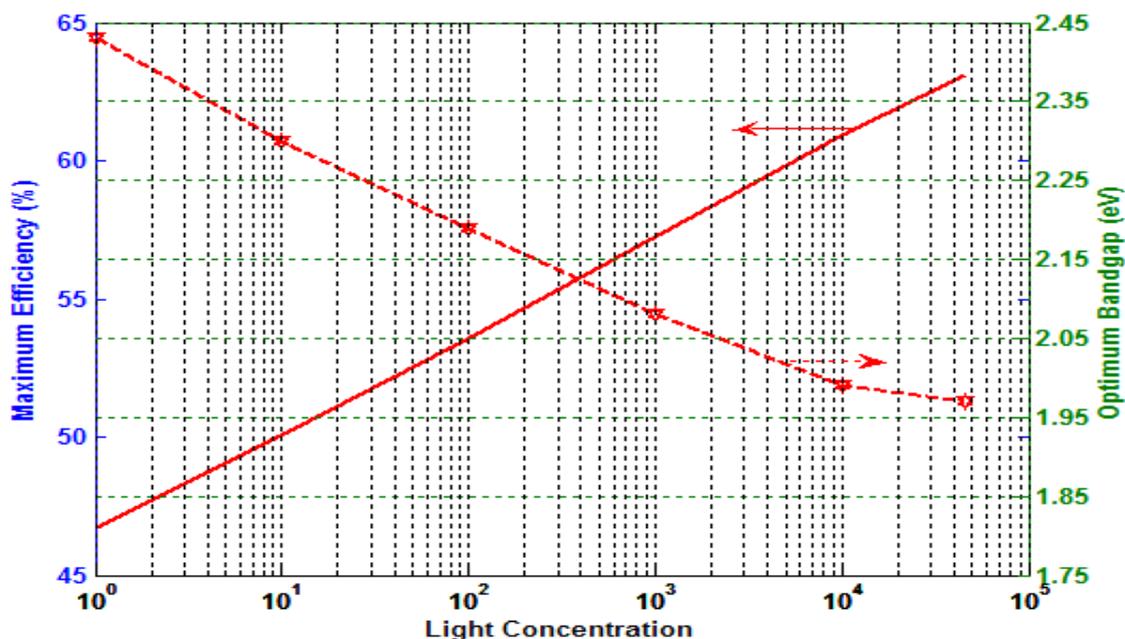
Fig. 4. Maximum efficiency and optimum bandgap energy,

E_{cv}, versus with entire light concentration for the one-IBSC It confirms the previous results and provides the all possibilities of maximum power efficiency at specified optimum bandgap energy. Of course, the change of incident solar light concentration will need different optimum bandgap energy. Also by investigating Fig. 4, one can recognize that when the solar light concentration increases, the maximum balanced power efficiency for the IBSC increases while the optimum bandgap energy, E_{cv}, decreases. From this behavior, it is clear that the bandgap energy of semiconductor material is inversely proportional to temperature under blackbody spectrum [38].

5. Quantum Dot Intermediate Band Solar Cell

For this type of solar cell, the size, shape, and spacing of the quantum dots in the barrier material are critical to improve the efficiency of the device. Whenever the QDs are arranged uniformly in the barrier material, the IBs are well-placed and the recombination is reduced [15]. Various techniques such as Metal Organic Chemical Vapor Deposition (MOCVP) and Molecular Beam Epitaxy (MBE) are available to produce highly uniform QD arrays in barrier material [38]. In this paper, the geometry of the QD is assumed cubic and thus it is characterized by one dimensional of cubic. Also, to simplify the analysis no valence band offset is assumed and the only confining potential occurs at the conduction band offset. Under these assumptions, the time-independent Schrödinger equation and the Krong-Penny model are used to calculate the energy bands in the QDs using the effective mass of charge carriers [10, 38, 39- 41]. $Al_{1-x}Ga_xAs/In_{1-x}Ga_xAs$ QDIBSC is

analysed theoretically to show the effect of QDs width size and the spacing between them in the barrier material on the efficiency. Here $Al_{1-x}Ga_xAs$ is the barrier ternary alloy and $In_{1-x}Ga_xAs$ is the QD ternary alloy. The energy bandgaps and effective masses of these alloys are calculated by the following chemical formulas [7, 42, 43]:

$Eg_{(Al1-xGaxAs)} = 3.099(1-x)+1.519x-0.2x(1-x)$, $\quad m^*_{(Al1-xGaxAs)}=(1-x)m^*_{(AlAs)}+ xm^*_{(GaAs)}$

$Eg_{(InxGa1-xAs)} = 1.519(1-x) + 0.417x - 0.588x(1-x)$, $m^*_{(InxGa1-xAs)} = (1-x)m^*_{(GaAs)}+ xm^*_{(InAs)}$

Here x (limited by $0 \leq x \leq 1$) is called the molar concentration for each GaAs and InAs in barrier and QD ternary alloys materials, respectively. There are two important steps in the study of this type of technology. (1) How to compound the semiconductor materials to obtain the required energy bandgaps. This step is studied in details in several researches [43- 46]. (2) Studying the effect of QDW and BT on the efficiency of solar cell and also knowing the permissible limits of them into the selected materials to obtain one-IB in the conduction band offset. More attention in this work is given to the second point. The semiconductors compound model used in this study of QDIBSC is $Al_{0.4}Ga_{0.6}As/In_{0.42}Ga_{0.58}As$ [44- 46]. The bandgap of ternary alloy $In_{0.42}Ga_{0.58}As$ (0.913eV) dot array material is smaller to that of the bandgap of ternary alloy $Al_{0.4}Ga_{0.6}As$ (2.103eV) barrier or bulk material to induce the one-IB by coupling of confined electronic states in the $In_{0.42}Ga_{0.58}As$ conduction band. The results of bandgap energies for the structure $Al_{0.4}Ga_{0.6}As/In_{0.42}Ga_{0.58}As$ QDIBSC are approximately close to the ideal values determined theoretically from Table 1 as in the previous section. Fig. 5 shows the changes of the one-IB energy when each of QDW and BT changes.
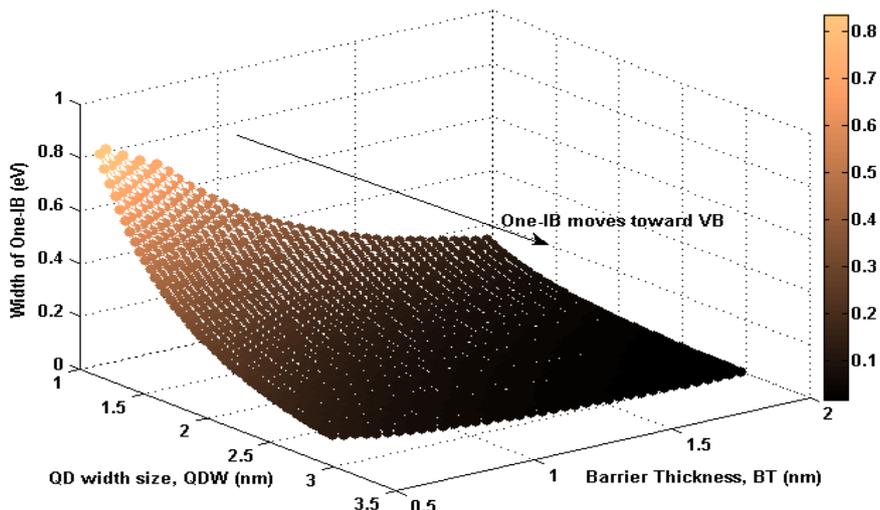
Fig. 5. The relation between width of one-IB energy and each of QDW and BT

It is clear that the larger values of QDW and BT tend to decrease the one-IB bandwidth and the later moves toward the valence band. Therefore, E_{ci} increases and E_{iv} decreases as shown in Figs. 6 and 7.
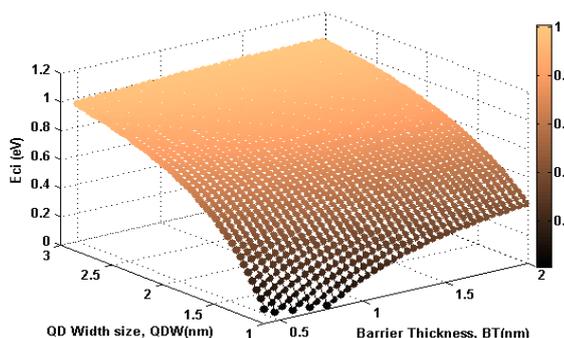

Fig. 6. Changing energy E_{ci} versus QDW and BT

This work concerns with the one-IB; therefore the QDW and BT in this type of ternary materials are limited with the values in Fig. 5, i.e., 1 nm ≤ QDW ≤ 3 nm and 0.5 nm ≤ BT ≤ 2 nm. The detailed balance efficiency for this structure under the above assumptions with changing QDW and BT, and thus E_{iv} and E_{ci}, at 1 sun and maximum light concentrations are plotted in Figs. 8 and 9. At first glance, when comparing the efficiency in Figs. 8, 9 and Table 2, with the results in Fig. 3 and Table 1, it is clear that the efficiency is approximately the same. This is due to the benefit from the ternary compound semiconductor materials. From the results of efficiency in Figs 8 and 9, the maximum power conversion efficiency of $Al_{0.4}Ga_{0.6}As/In_{0.42}Ga_{0.58}As$ QDIBSC as a function of QDW and BT or E_{vi} and E_{ci} is changed from 45.32% to 62.81% at 1 sun and maximum light concentrations, respectively.

When one compares these values with the previous results in the one-IBSC, it is clear that the values are smaller by a little bit. This is natural because we are limited by the selected QDIBSC materials. Also, one can notice that the coverage or matching areas are probably small. So the movement in QDW range that is covered by the defined BT range has become narrower. When QDW decreases towards a lower limit, BT increases to an upper limit. Another thing to notice from these curves is that the maximum balanced efficiencies QDIBSC behave the same trend as in an ideal case, one-IBSC. That means that it realizes current-matching easily for 1 sun compared to the maximum light concentration, which is very difficult. Table 2 summarizes the maximum efficiency and optimum QDW and BT of QDIBSC at 1 sun and maximum light concentrations.
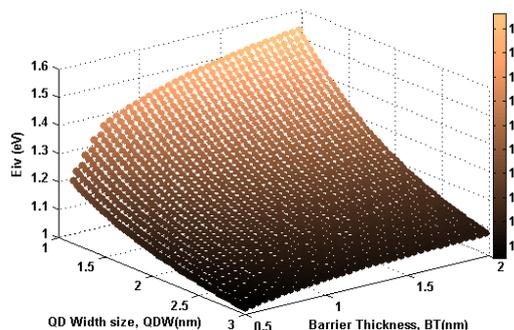

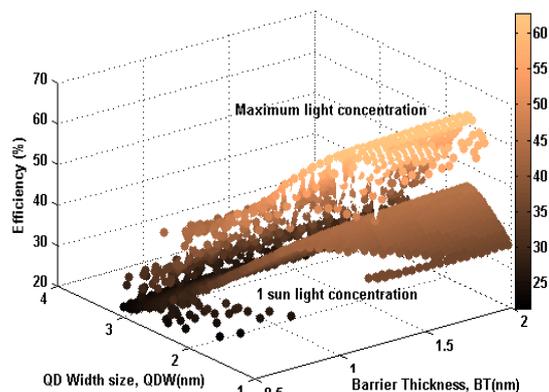**Fig. 7.** Changing energy E_{iv} versus QDW and BT

Fig. 8. Detailed balance efficiency of QD solar cell one- IB varies with QDW and BT at blackbody spectrum under 1 sun and maximum light
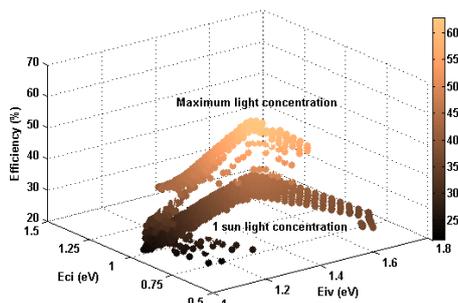
1090

Fig. 9. Detailed balance efficiency of QD solar cell one- IB varies with E_{iv} and E_{ci} at blackbody spectrum under 1 sun and maximum light concentrations

Table 2. Summarizes the maximum efficiency and optimum BT and QDW of QDIBSC at 1 sun and maximum light concentrations for the blackbody spectrum

Solar Spectrum	1 Sun Concentration				Max. Concentration			
	Max. Efficiency (%)	Opt. BT & QDW (nm)		IB Width (eV)	Max. Efficiency (%)	Opt. BT & QDW (nm)		IB Width (eV)
		BT	QDW			BT	QDW	
Blackbody	45.32	1.98	1.60	0.0696	62.81	1.94	1.64	0.0684

6. Conclusion

In this article, the detailed balance efficiency of nanostructured solar cell dependent on Shockley and Queisser design model has been studied under the standard blackbody spectrum. For the nanostructured solar cell, the analyses of detailed balance efficiency showed that it varies with the place of the one-IB within the bandgap energy of the bulk semiconductor. Therefore, the optimum location of one-IB that provides the maximum power conversion efficiency can be determined. Accordingly, the QDIBSC is investigated to achieve the results of one-IBSC. By utilizing the Schrödinger equation and the Krong-penny model, the relation between QDIBSC parameters, (QDW and BT), and detailed balance efficiency for achieving maximum efficiencies are defined. The results have shown that both the location of the one-IB and the maximum power conversion efficiency strongly depend on the considered parameters. The maximum efficiencies are changed from 46.74% and 63.13% for one-IBSC to 45.32% and 62.81% for $Al_{0.4}Ga_{0.6}As/In_{0.42}Ga_{0.58}As$ QDIBSC under the 1 sun and maximum light concentrations; respectively. In the QDIBSC, it is very difficult to obtain the current-matching. In future work, increasing the energy bands to two-IB in QDIBSC to improve the efficiency will be considered.

References

[1] P. Balaji, B. M. Babu, and A. Shafarna, "Modeling of Solar Cell Using Odd Size Quantum Dots", International Journal on Advanced Electrical and Electronics Engineering, IJAEEE, Vol. 1, Issue 1, 2012.

[2] K. Sablon, J. Little, V. Mitin, A. Sergeev, N. Vagidov, and K. Reinhardt, "Strong Enhancement of Solar Cell Efficiency Due to Quantum Dots with Built-In Charge", NanoLett., 11, pp. 2311-2317, 2011.

[3] K. Yoshida, Y. Okada, and N. Sano, "Device Simulation of Intermediate Band Solar Cells: Dependence on Number of Intermediate Band Layers", 38th Photovoltaic Specialists Conference (PVSC), IEEE, pp. 1669 – 1672, 2012.

[4] K. Tanabe, D. Guimard, D. Bordel, R. Morihara, M. Nishioka, and Y. Arakawa, "High-Efficiency InAs/GaAs Quantum Dot Solar Cells by MOCVD", 38th Photovoltaic Specialists Conference (PVSC), IEEE, pp. 1929 – 1930, 2012.

[5] C. Lin, W. Liu, and C. Yu Shih, "Detailed balance model for intermediate band solar cells with photon conservation", Optics Express, Vol. 19, Issue 18, pp. 16927 – 16933, 2011.

[6] S. P. Bremner, A. Pancholi, K. Ghosh, S. Dahal, G. M. Liu, K. Y. Ban, M. Y. Levy, and C. B. Honsberg, "Growth of InAs Quantum Dots on GaAsSb for the Realization of a Quantum Dot Solar Cell", 33rd

Photovoltaic Specialists Conference (PVSC), IEEE, pp. 1 - 6, 2008.

[7] D. Qing-Wen, W. Xiao-Liang, Y. Cui-Bai, X. Hong-Ling, W. Cui-Mei, Y. Hai-Bo, H. Qi-Feng, B. Yang, L. Jin-Min, W. Zhan-Guo, and H. Xun, "Computational Investigation of InxGa1-xN/InN Quantum-Dot Intermediate-Band Solar Cell", Chinese Physics Letters, Vol. 28, No. 1, 2011.

[8] P. G. Linares, A. Marti, E. Antolin, I. Ramiro, E. Lopez, C. D. Farmer, C. R. Stanley, and A. Luque, "Low-Temperature Concentrated Light Characterization Applied to Intermediate Band Solar Cells", IEEE Journal of Photovoltaics, Vol. 3, No. 2, 2013.

[9] D. Farrell, Y. Takeda, K. Nishikawa, T. Nagashima, T. Motohiro, N. Ekins-Daukes, and Y. Okada, "A NEW TYPE OF HOT-CARRIER SOLAR CELL UTLISING THERMAL UP AND DOWN CONVERSION OF SUNLIGHT", Appl. Phys. Lett. 99, 111102, 2011.

[10] Q. Xiaosheng, Z. Sisi, B. Hongyin, and X. Liling, "The effect of InAs quantum-dot size and interdot distance on GaInP/GaAs/GaInAs/Ge multi-junction tandem solar cells", Journal of semiconductor, Vol. 34, No. 6, pp. 062003-1 - 062003-5, 2013.

[11] E. O. Chukwuocha, and M. C. Onyeaju, "Effect of Quantum Confinement on the Wavelength of CdSe, ZnSand GaAs Quantum Dots (Qds)", International Journal of Scientific & Technology Research, Vol. 1, Issue 7, 2012.

[12] E. Antolin, A. Marti, and A. Luque, "The Lead Salt Quantum Dot Intermediate Band Solar Cell", 37th Photovoltaic Specialists Conference (PVSC), IEEE, pp. 1907-1912, 2011.

[13] L. Kosyachenko, "Solar Cells – New Aspects and Soluations", InTech, Online published, ISBN 978-953-307-761-1, 2011.

[14] A. Ogura, T. Morioka, P. Garcia, E. Hernandez, I. Ramiro, E. Antolin, A. Marti, A. Luque, M. Yamaguchi, and Y. Okada, "Modelling of Quantum Dot Solar Cells for Concentrator PV Applications", 37th Photovoltaic Specialists Conference (PVSC), IEEE, pp. 2642 - 2645, 2011.

[15] J. Ojajarvi, "Tetrahedral chalcopyrite quantum dots in solar-cell applications", Msc., Jyvaskyla University, Finland, 2010.

[16] E. J.Steven, "Quantum Dot Intermediate Band Solar Cells: Design Criteria and Optimal Materials", PhD, Drexel University, Philadelphia, Pennsylvania, USA, 2012.

[17] N. G. Anderson, "On quantum well solar cell efficiencies", Physica E, 14, pp. 126 - 131, 2002.

[18] A. Luque and A. Marti, "Thermodynamic consistency of sub-bandgap absorbing solar cell proposals", IEEE Transactions on Electron Devices, 49, pp. 2118 – 2124, 2001.

[19] W. van Roosbroeck, W. Shockley, "Photon-Radiative Recombination of Electrons and Holes in Germanium", Phys. Rev. 94, pp. 1558-1560, 1954.

[20] A. Marti, L. Cuandra, and A. Luque, "Quantum dot intermediate band solar cell", 28th IEEE PVSC, pp. 940 – 943, 2000.

[21] A. Luque, A. Mart, "Increasing the Efficiency of Ideal Solar Cells by Photon Induced Transitions at Intermediate Levels", Phys. Rev. Lett. 78, 1997.

[22] A. Mart, E. Antolin, C. R. Stanley, C. D. Farmer, N. Lopez, P. Diaz, E. Canovas, P. G. Linares, A. Luque, "Production of photocurrent due to intermediate to conduction band transitions: a demonstration of a key operating principle of the intermediate band solar cell", Physical Review Letters 97, 2006.

[23] A. Luque, A. Mart, "The intermediate band solar cell: progress toward the realization of an attractive concept", Advanced Materials 22, pp. 160-174, 2010.

[24] A. Luque, A. Mart, C. Stanley, "Understanding intermediate band solar cells", Nature Photonics 6, 2012.

[25] Y. Okada, T. Morioka, K. Yoshida, R. Oshima, Y. Shoji, T. Inoue, T. Kita, "Increase in photocurrent by optical transitions via intermediate quantum states in direct doped InAs/GaNAs strain compensated quantum dot solar cell", Journal of Applied Physics 109, 2011.

[26] A. Mart, D. Fuertes Marron, A. Luque, "Evaluation of the efficiency potential of intermediate band solar cells based on thin film chalcopyrite materials", Journal of Applied Physics 103, 2008.

[27] D. Fuertes Marron, A. Mart, A. Luque, "Thin-film intermediate band chalcopyrite solar cells", Thin Solid Films 517, 2009.

[28] A. Luque, A. Mart, N. Lopez, E. Antolin, E. Canovas, C. Stanley, C. Farmer, P. Diaz, "Operation of the intermediate band solar cell under nonideal space charge region conditions and half filling of the intermediate band", Journal of Applied Physics 99, 2006.

[29] A. Mart, L. Cuadra, A. Luque, "Quasi-drift diffusion model for the quantum dot intermediate band solar cell", IEEE Transactions on Electron Devices 49, 2002.

[30] K. Tanabe, K. Watanabe, Y. Arakawa, Thin film InAs/GaAs quantum dot solar cells layer transferred onto Si substrates and flexible plastic films", 38th IEEE PVSC, 2012.

[31] A. Mart, N. Lopez, E. Antolin, E. Canovas, A. Luque, C. R. Stanley, C. D. Farmer, P. Diaz, "Emitter degradation in quantum dot intermediate band solar cells", Applied Physics Letters 90, 2007.

[32] S. M. Hubbard, C. G. Bailey, C. D. Cress, S. Polly, J. Clark, D. V. Forbes, R. P. Raffaelle, S. G. Bailey, C. M. Wilt, "Short circuit current enhancement of GaAs solar cells using strain compensated InAs quantum dots", 33rd IEEE PVSC, pp. 1-6, 2008.

[33] S. M. Hubbard, C. D. Cress, C. G. Bailey, R. P. Raffaelle, S. G. Bailey, D. M. Wilt, "Effect of strain compensation on quantum dot enhanced GaAs solar cells", Applied Physics Letters 92, 2008.

[34] K. Akahane, N. Yamamoto, T. Kawanishi, "Fabrication of ultra high density InAs quantum dots using the strain compensation technique", Physica Status Solidi A 208, 2011.

[35] W. Shockley and H.J. Queisser, "Detailed balance limit of efficiency of *p-n* junction solar cells", J. Appl. Phys. 32, pp. 510-519, 1961.

[36] C. Linge, "Modeling of the Intermediate Band Tandem Solar Cell Using the AM1.5 Spectra", MSc. Thesis, Department of Physics, University of Science and Technology, Norwegian, 2011.

[37] A. Kurome, R. Morigaki, S. Souma, and M. Ogawa, "Analysis of Electronic Structure in Quantum Dot Arrays for Intermediate Band Solar Cells", IMFEDK, Kansai, pp. 114-115, 2011.

[38] R. Aguinaldo, "Modeling Solutions and Simulations for Advanced III-V Photovoltaics Based on Nanostructures", M.Sc in Materials Science & Engineering, College of Science, Rochester Institute of Technology, Rochester, NY, 2008.

[39] A. Aly, A. Nasr, "Theoretical Performance of Solar Cell based on Mini-bands Quantum Dots", Journal of Applied Physics, Volume 115, Issue 114311, 2014.

[40] M. Y. Levy, C. Honsberg , A. Marti, and A. Luque, "Quantum dot intermediate band solar cell material systems-with negligible valence band offsets", Photovoltaic Specialists Conference, 31st IEEE, 2005.

[41] S. P. Day, "The Kronig-Penney Approximation: May It Live On", IEEE Transactions on Education, Vol. 33, No. 4, 1990.

[42] M. Ferhat, "Computational Optical bandgap Bowing of III-V Semiconductors Alloys", Phys. Stat. Sol., Vol. 241, No. 10, pp. 38-41, 2004.

[43] I. Vurgaftman, J. R. Meyer, and L. R. Ram-Mohan, "Band Parameters for III-V Compound Semiconductors and their Alloys", Journal of Applied Physics, Vol. 89, No. 11, pp. 5815 – 5875, 2001.

[44] V. Popescu, G. Bester, M. Hanna, A. Norman, and A. Zunger, "Theoretical and experimental examination of the intermediate-band concept for strain-balanced (In,Ga)As/Ga(As,P) quantum dot solar cells", Physical review B 78, pp. 205321(1-17) , 2008.

[45] A. Kechiantz, A. Afanasev, and J. Lazzan, "Modification of band alignment at interface of Al$_y$Ga$_{1-}$ $_y$Sb/Al$_x$Ga$_{1-x}$As type-II quantum dots by concentrated sunlight in intermediate band solar cells with separated absorption and depletion regions", SPIE Photonics West, San Francisco, CA, USA, 2013.

[46] S. Lade, and A. Zahedi, "A revised ideal model for AlGaAs/GaAs quantum well solar cells", Microelectronics Journal 35, pp. 401-410, 2004.